Characterization of Silicon Nanoparticles Prepared from Porous Silicon

Richard A. Bley,[†] Susan M. Kauzlarich,*[,†] Jeffrey E. Davis,[‡,§] and Howard W. H. Lee[‡]

Department of Chemistry, University of California, Davis, California 95616; Lawrence Livermore National Laboratory, Livermore, California 94550; and Department of Applied Science, University of California, Davis, California 95616

Received December 18, 1995. Revised Manuscript Received March 13, 1996[⊗]

Nanometer-sized silicon particles have been produced by ultrasonic dispersion of thin sections of porous silicon (PS) in organic solvents. The particles have been characterized by HRTEM (high-resolution transmission electron microscopy), FTIR (Fourier transform infrared) spectroscopy, and fluorescence spectroscopy. HRTEM shows both aggregates of and monodispersed crystallite particles of Si. The larger aggregates range in size from 20 to 50 nm and are made up of small crystallites with diameters of 2−10 nm. Monodispersed crystallites ranged in size from 2−10 nm. All the particles have an amorphous layer of SiO_2. The photoluminescence (PL) spectrum shows two peaks: a red peak at around 680 nm, which is typical for PS and a blue peak between 415 and 446 nm, which is not typical for as-prepared PS. As a function of increased excitation intensity, the blue peak grows at the expense of the red. This is discussed in light of photoluminescence lifetime data. The red luminescence is attributed to quantum confinement. The blue luminescence is attributed to either extremely small Si crystallites or $(Si(II))^0$ defects embedded in the oxide matrix.

Introduction

During the past few years extensive research into the synthesis of semiconductor nanoclusters has occurred. This is primarily due to the unusual optical, electronic, and mechanical properties these materials possess.[1] Many of these properties are attributed to quantum confinement effects which occur when the size of the cluster becomes smaller than the exciton diameter of the bulk semiconducting material. Until recently, the synthesis of nanometer-sized Si clusters has not been pursued as vigorously as the II−VI and III−V semiconductors. One reason for this is the greater difficulty involved in synthesizing discrete nanosized Si clusters. In addition, the indirect bandgap possessed by bulk crystalline Si inhibits light emission from electron/hole pair recombination. This inhibition of light emission would make nanoclusters of Si unsuitable for applications in optoelectronic devices.

Interest in preparing Si nanoclusters is fueled by the suggestion that the room temperature luminescence of porous silicon (PS) results from quantum confinement.[2,3] The idea that Si could be made to luminesce, perhaps even efficiently, has produced a great deal of interest in the synthesis and characterization of both porous silicon and silicon nanoclusters. Much of this interest arises from the possibility of producing an inexpensive and uncomplicated interface bridging the two economically important technologies: digital computing, done electronically using Si integrated circuits, and digital communication, done optically using silica (SiO_2) single-mode fibers.[3]

Production of luminescent colloidal suspensions of Si nanoparticles from PS by ultrasonic fracture,[4−6] provides an opportunity to investigate the mechanism involved in PS luminescence. It is still unclear whether this is due solely to quantum confinement of the electron and its respective hole, the so-called particle in a box condition, or if this includes some other condition or set of conditions such as surface states or the presence of other silicon compounds such as siloxene ($Si_6O_3H_6$).[7−10] Some of the methods used to synthesize Si nanoclusters include thermal pyrolysis,[11] evaporation and laser ablation into an inert atmosphere,[12−15] and high-pressure solution-phase synthesis.[16] Generally a wide size range is obtained with these methods, including the technique of ultrasonic fracturing.[4] To date, the technique that has produced Si nanoclusters of the most uniform size involves a high-temperature pyrolysis

[†] Department of Chemistry.
[‡] Lawrence Livermore National Laboratory.
[§] Department of Applied Science.
[⊗] Abstract published in *Advance ACS Abstracts,* July 15, 1996.

(1) Siegel, R. W. *Mater. Sci. Eng. A* **1993**, *168*, 189.
(2) Canham, L. T. *Appl. Phys. Lett.* **1990**, *57*, 1046.
(3) Brus, L. *J. Phys. Chem.* **1994**, *98*, 3575.
(4) Heinrich, J. L.; Curtis, C. L.; Credo, G. M.; Kavanagh, K. L.; Sailor, M. J. *Science* **1992**, *255*, 66.
(5) Bley, R. A.; Kauzlarich, S. M.; Lee, H. W. H.; Davis, J. E. *Mater. Res. Soc. Symp. Proc.* **1994**, *351*, 275.
(6) Lee, H. W. H.; Davis, J. E.; Olsen, M. L.; Kauzlarich, S. M.; Bley, R. A.; Risbud, S.; Duval, D. *Mater. Res. Soc. Symp. Proc.* **1994**, *351*, 129.
(7) Hamilton, B. *Semiconduct. Sci. Technol.* **1995**, *10*, 1197.
(8) Prokes, S. M. *J. Appl. Phys.* **1993**, *73*, 407.
(9) Fuchs, H. D.; Brandt, M. S.; Stutzmann, M.; Weber, J. *Mater. Res. Soc. Symp. Proc.* **1992**, *256*, 159.
(10) Sailor, M. J.; Kavanagh, K. L. *Adv. Mater.* **1992**, *4*, 432.
(11) Wu, J. J.; Flagan, R. C. *J. Appl. Phys.* **1987**, *61*, 1365.
(12) Hayashi, S.; Tanimoto, S.; Yamamoto, K. *J. Appl. Phys.* **1990**, *68*, 5300.
(13) Okada, R.; Ijima, S. *Appl. Phys. Lett.* **1991**, *58*, 1662.
(14) Ijima, S. *Jpn. J. Appl. Phys.* **1987**, *26*, 357.
(15) Saito, Y. *J. Cryst. Growth* **1979**, *47*, 61.
(16) Heath, J. R. *Science* **1992**, *258*, 1131.

S0897-4756(95)00608-9 CCC: $12.00

Table 1. Parameters Used To Prepare Colloidal Si from PS[a]

sample no.	hf (%)	ethanol (%)	current density (ma/cm^2)	anodization time (min)	colloid solvent	sonication time (days)
1	20	0	20	20	acetonitrile	1
2	20	0	20	20	acetonitrile	2
3	20	0	20	20	acetonitrile	5
4	20	0	20	20	acetonitrile	7
5	20	10	20	20	acetonitrile	7
6	20	10	20	20	toluene	7
7	20	30	20	20	acetonitrile	7
8	20	30	20	20	toluene	7
9	20	30	5	180	acetonitrile	7
10	20	30	7.5	180	acetonitrile	7
11	20	60	5	180	acetonitrile	7

[a] All samples were prepared using Al-backed p-type (B-doped) (100) oriented Si wafers with resistivity of 14−22 Ωcm.

where the Si clusters are prepared as an ethylene glycol colloid.[17]

The brief report on the production of Si nanoclusters from ultrasonic fracturing of PS indicated that there was a large range of particle sizes in the colloid.[4] It was suggested that this method of synthesis avoided the contamination of SiO_2 and thus provides greater options for studying the properties of Si nanoclusters. We were interested in optimizing the production of Si nanoclusters by this method and investigating their optical properties. We have investigated the effects of electrolyte composition, anodization time used in the preparation of PS, and ultrasonication time on the production of Si particles. Thin sections of PS are ultrasonicated for longer times and should provide a more narrow distribution of sizes compared to previously published work.[4] We have also used a 20 nm sieve to remove larger crystallites from the colloids. This paper describes the HRTEM, FTIR, and PL data of Si colloids prepared from PS and compares these results with Si colloids prepared by other methods.

Experimental Section

The PS samples were formed by anodizing p-type (B-doped) (100) oriented silicon wafers with resistivity of 14−22 Ω cm in 20% HF solutions. Anodization took place over 20 or 180 min with a constant current density of 5, 7.5, or 20 mA/cm^2. 20% HF solutions contained 0, 10, 30, or 60% ethanol by weight with a corresponding amount of water making up the remainder of the solution. With some samples a second electrochemical etch was performed using a 1% solution of HF/H_2O with a current density of 160 mA/cm^2 for 1 min to separate the anodized PS layer from the Si substrate.

The samples were then rinsed with deionized water and dried under a stream of N_2 gas and placed in a vacuum chamber. The chamber was evacuated to 70 mTorr for several hours to help facilitate the removal of water, and subsequently the samples were brought into a solvent-free drybox. The PS was mechanically removed from the Si substrate. The resulting material was collected in a sidearm Schlenk flask. Approximately 10 mL of solvent (acetonitrile or toluene) which had been dried over calcium hydride, distilled, and degassed was added to the flask containing the PS. The mixture was placed in a Branson Ultrasonic bath (50/60 Hz) for up to 7 days. Cyclohexane was also investigated as a possible solvent, but did not appear to support a colloid, and its use as a solvent was not investigated further. Generally, upon removal from the ultrasonic bath the solution was allowed to settle and the resulting supernatant was removed for study. For several samples the supernatant was put through a 20 nm inorganic membrane filter (Anotop 10 from Whatman) and the resulting filtrate was used for study. Conditions for the preparation of each sample are provided in Table 1.

UV−vis spectra were obtained from the solutions several times during their sonication with a Hewlett-Packard 8450A diode-array spectrophotometer. FTIR spectra were taken of the PS powders before sonication in the form of a KBr pellet. An equal mass of KBr was used as a reference. IR spectra of the colloid solutions were obtained both by evaporation of the colloid solvent on a CsI salt plate and from a solution cell made of two KBr salt plates. The spectra were collected on a Mattson Galaxy series FTIR 3000.

HRTEM samples were prepared by evaporation of the colloid solution on lacy carbon-coated electron microscope grids. The electron microscope was a JEOL 200CX HREM which operated with an accelerating voltage of 200 kV.

A Ti:sapphire laser and Xe arc lamp were used as sources for optical excitation in the photoluminescence studies and are described more fully elsewhere.[6] For several samples, photoluminescence spectra were collected for both the colloidal solution and the PS used to make the solution.

Results and Discussion

Materials Processing and HRTEM. Table 1 shows the conditions used in the preparation of the PS colloid. The addition of ethanol to our electrolyte solution and the increase in anodization times were expected to produce more uniform crystallites in the size range of 10 nm or less, the exciton diameter of Si. Previous HRTEM studies[18] carried out on the PS colloid samples made with HF and water were reported to have a wide range of particle sizes (20−50 nm) and shapes with few particles in the smaller size ranges. Subsequent studies done on the same samples, however, reveal that smaller crystallites (between 2 and 20 nm) are much more prevalent than was reported. The initial inability to observe these smaller crystallites is attributed to their small size, which allows them to fall through the holes on the carbon grid as they were being deposited for study. The samples prepared with ethanol in the anodization step also produce a significant fraction of the smaller nanometer-sized particles with the overall sizes ranging from 2 and 40 nm. For all samples, lattice fringes for individual crystallites smaller than 7 nm have not been resolved. The smaller crystallites adhere to the grid only in areas absent of holes, and diffraction patterns of these particles have not been obtained.

All the colloid solutions are fairly similar in appearance based on HRTEM micrographs and the colloid

(17) Littau, K. A.; Szajowshki, P. J.; Muller, A. J.; Kortan, A. R.; Brus, L. E. *J. Phys. Chem.* **1993**, *97*, 1224.

(18) Berhane, S.; Kauzlarich, S. M.; Nishimura, K.; Smith, R. L.; Davis, J. E.; Lee, H. W. H.; Olson, M. L. S.; Chase, L. L. *Mater. Res. Soc. Symp. Proc.* **1993**, *298*, 99.

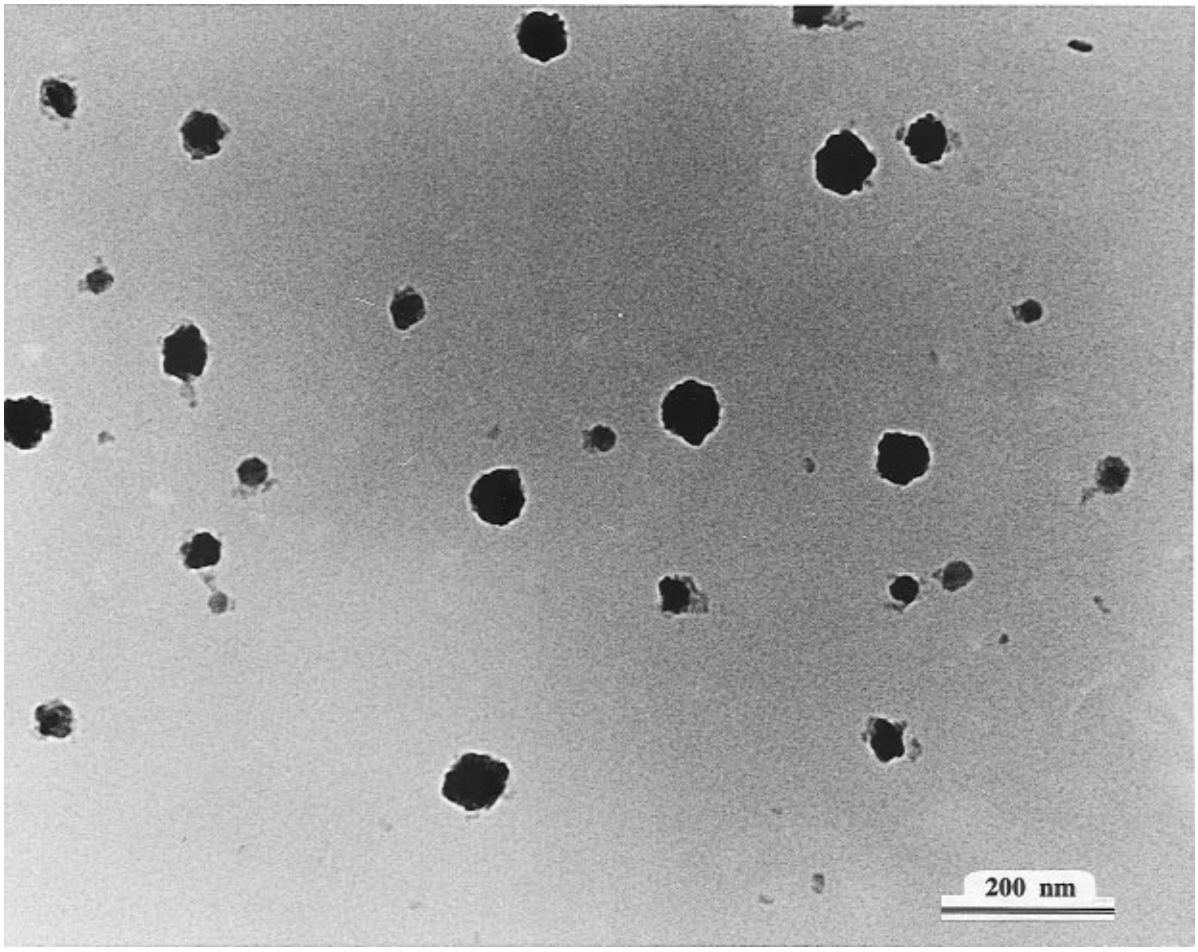

Figure 1. High-resolution TEM micrograph of a colloidal solution.

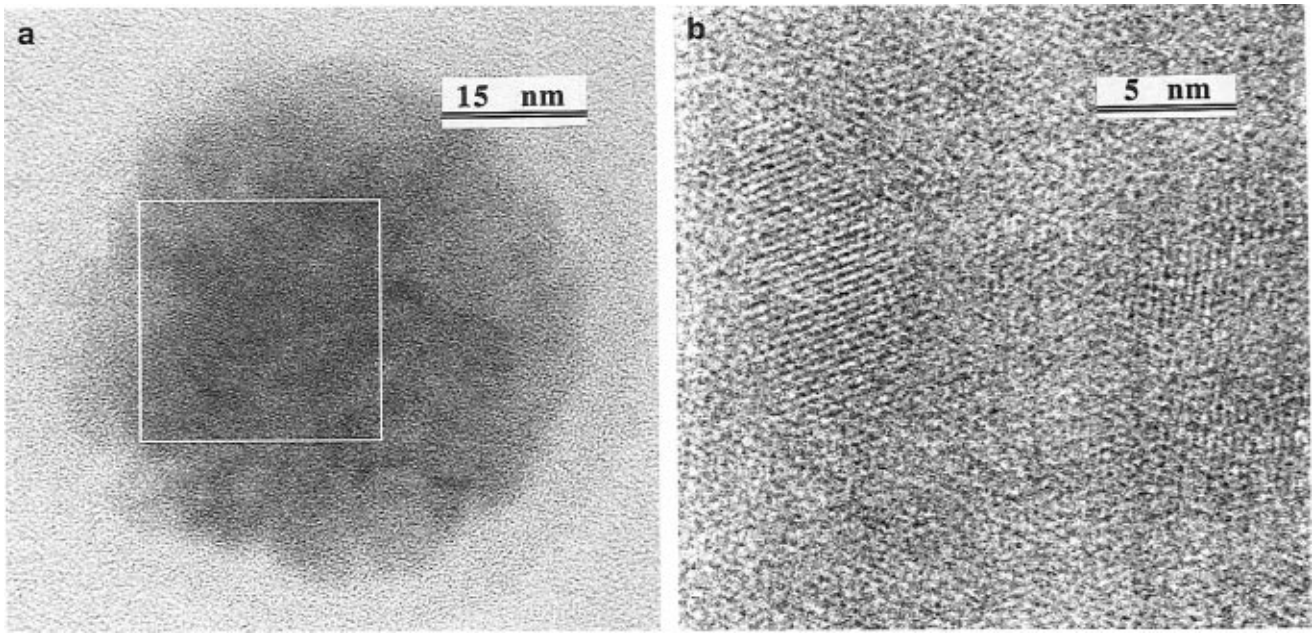

Figure 2. (a) High-resolution TEM micrograph of a typical cluster of Si crystallites with an outer amorphous layer between 3 and 4 nm and (b) an enlargement of the outline region shown in (a). The lattice spacing of 0.31 nm indicates this is a view down a ⟨110⟩ axis showing the {111} interplanar spacing.

solution (no. 11) made from PS produced with 60% ethanol in the electrolytic solution, a 5 mA/cm^2 current density, and an anodization time of 180 min will be discussed in detail. Figure 1 shows an electron micrograph illustrating the sizes and shapes of particles observed in this colloid. Figure 2 shows one of the larger particles from this colloidal solution as well as an enlargement of a section. The particle has a diameter of approximately 40 nm. The differences in the orientations of the lattice fringes suggest that this is not a single crystallite but an agglomeration of several small crystallites. This interpretation is in agreement with

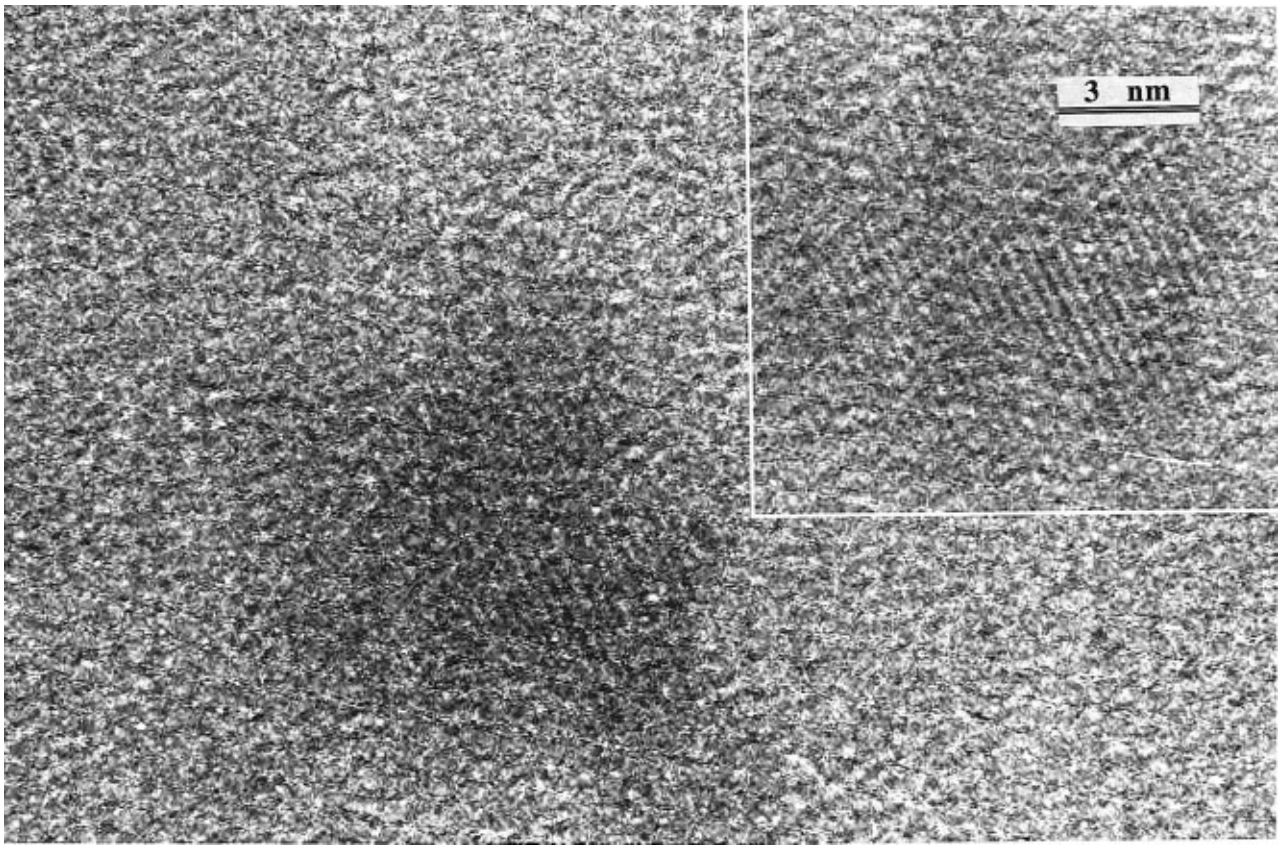

Figure 3. High-resolution TEM micrograph of an individual Si nanocrystal. Inset: an enlargement of the cluster, clearly showing the lattice spacing of 0.31 nm.

the electron diffraction pattern for this particle which shows diffraction spots arising from several crystallites of Si having different crystallographic orientations. The lattice fringes of the larger crystallites, approximately 7−11 nm in diameter, making up the particle can be clearly seen in Figure 2. The smallest crystallites in the agglomeration are about 2 nm. In addition, an amorphous layer surrounds the entire agglomeration, demonstrating that a separate morphology exists at its surface. This picture typifies the general structure of the larger particles in that they are made up of small crystallites which have agglomerated together to make a cluster. Whether it is chemical bonding or van der Waals forces holding the clusters together is difficult to ascertain. However, similar formations were found after passing the solution through a 20 nm inorganic sieve, suggesting that these clusters are formed in solution and not simply a piece of the PS starting material.

In addition to these relatively large agglomerations of crystallites, small individual crystallites are also observed. Figure 3 shows an electron micrograph of a crystallite that is approximately 8 nm in diameter. The lattice spacing of 0.31 nm suggests that the {111} planes are responsible for the visible fringes in the micrograph. There is no amorphous layer visible for the crystallites ranging in size from 2 to 10 nm in diameter. This is probably due to the smaller amount of amorphous material that the beam travels through relative to the amorphous background of the carbon grid.

As mentioned above, for several colloids, a 20 nm inorganic membrane filter was used to remove Si particles greater than 20 nm in diameter. The colloid appears to be very similar to those described above except that the crystallites are widely separated within an amorphous casing. The presence of the agglomerations in these solutions suggests that the Si crystallites can associate and dissociate in solution. The amorphous casing is attributed to a surface of silicon oxide covering the crystallites.

It is possible that passing the colloid through the sieve increases the exposure to oxygen and further oxidizes the small crystallites which then agglomerate in solution. The larger crystallites have a lattice spacing of 0.31 nm, consistent with the spacing between the [111] planes in Si. These agglomerates of crystallites must form after going through the sieve since most of them are larger than 20 nm.

FTIR. Detailed IR experiments on the different PS samples were carried out before and after ultrasonification to help determine the composition of the amorphous surface layer. The PS, removed from the wafer, was mixed with ground KBr and pressed into a pellet. Figure 4 shows the IR spectra of a PS sample (no. 9) made from an electrolytic HF solution having 30% ethanol, a current density of 5 mA/cm^2, and an anodization time of 180 min. One spectrum (as prepared) was taken after the sample was in a solvent free drybox for 24 h. The other spectrum (after sonication) is of the sonicated colloidal Si suspension, after evaporation of the solvent, on a CsI salt plate. The three prominent features in the "as prepared" spectrum are the Si−H stretching at 2073 cm^{-1} and the Si−H bending and wagging modes at 902 and 661 cm^{-1} respectively.[19] In the spectrum labeled "after sonication", the Si−H peaks

(19) Gupta, P.; Colvin, V. L.; George, S. M. *Phys. Rev. B* **1988**, *37*, 8234.

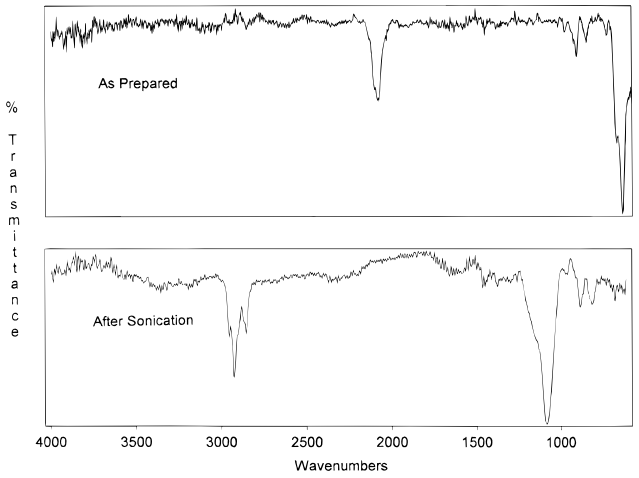

Figure 4. FTIR spectra of PS samples: (a) spectrum of the PS sample before ultrasonication; (b) spectrum of the colloid, after evaporation of solvent. The sample was made with 30% ethanol in the HF solution. A current density of 5 mA/cm^2 was used with an anodization time of 180 min. The sample was ultrasonicated for 5 days in acetonitrile.

have disappeared completely and new peaks arise in the hydrocarbon region of the spectrum around 2958, 2927, and 2856 cm^{-1}. In addition, a Si−O stretching peak at 1087 cm^{-1} is present. It has been suggested that the hydrocarbon peaks which often appear in IR spectra of PS samples are due to alcohol (generally ETOH) residue left by the electrolytic solution.[20] As can be seen in Figure 4, no such peaks are present for the PS sample prepared with HF/ETOH. These three peaks in the hydrocarbon region of the spectrum are also present in our PS samples made only with HF and water after brief periods of exposure to air and, therefore, are not due to the use of alcohol in the anodization step. We have found that after only brief exposure to air the PS samples show hydrocarbon contamination, even when alcohol is not used in the anodization process. The appearance of these hydrocarbon peaks is greatly slowed if the PS sample is kept in a solvent-free drybox under N_2. However, these peaks eventually begin to appear even under solvent-free conditions. This pattern of Si−H peak disappearance along with Si−CH_3 and Si−O peak appearance is seen for all PS samples regardless of the anodization conditions. The "after sonication" FTIR spectrum is also typical for samples which were filtered with the 20 nm inorganic filter membrane. The samples were monitored by IR over time and intermediate spectra where both sets of peaks are present were collected. IR spectra of the acetonitrile colloid show an -OH stretch in addition to the Si−CH_x (x = 1−3) and Si−O peaks. This alcohol must be produced in the colloid solution during the sonication step. At the present time, it appears that even under dry anaerobic conditions O_2 and/or H_2O are still present in large enough amounts to passivate the surface of the Si nanocluster with oxide and hydroxide in the colloid solution. It is probable that Si−O and Si−OH bonds are formed by the combination of very small concentrations of O_2 and H_2O present in the solvent plus the high-temperature produced in ultrasonication.

UV−Vis Absorbance. An absorption spectrum of a colloid (no. 5) is shown in Figure 5 and is typical for

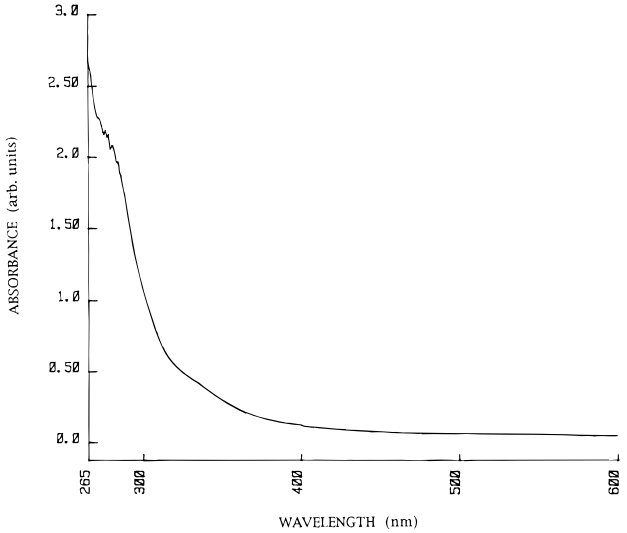

Figure 5. UV−vis spectrum of a typical PS colloid in acetonitrile.

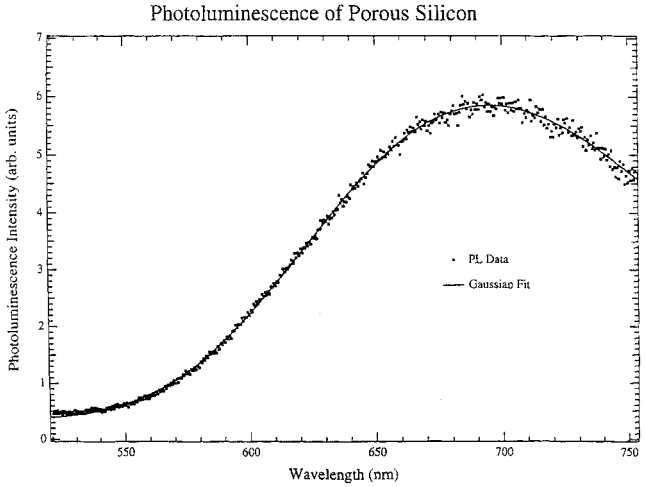

Figure 6. Photoluminescence spectra of PS along with Gaussian line shape fit. Excitation provided by 400 nm laser pulses.

all of the colloids. The spectrum is consistent with the small size of the observed Si crystallites and is similar to those reported for 3−8 nm, surface-oxidized Si crystallites.[17] A plot of the square root of the absorption as a function of absorption energy shows that the onset of the optical transition remains indirect, despite the reduced size of the particles. In addition, a direct transition occurs at ∼3.4 eV, which is also observed in bulk Si. These properties have also been observed in Si nanocrystals generated from high-temperature aerosols[21] and cast doubt on the theory that quantum confinement in indirect semiconductors gives rise to a more direct optical transition.

Photoluminescence. Figure 6 shows the low excitation intensity photoluminescence (PL) spectrum of a PS sample while still on the Si wafer substrate. It shows a peak near 695 nm that is blue-shifted from that in bulk Si. This has led to explanations invoking quantum confinement. A fit of the PL spectrum to a Gaussian line shape is included and shows excellent agreement. This spectrum is fairly typical for PS, and

(20) Borghesi, A.; Sassella, A.; Pivac, B.; Pavesi, L. *Solid State Commun.* **1993**, *87*, 1.

(21) Brus, L. E.; Szajowski, P. F.; Wilson, W. L.; Harris, T. D.; Schuppler, S.; Citrin, P. H. *J. Am. Chem. Soc.* **1995**, *117*, 2915.

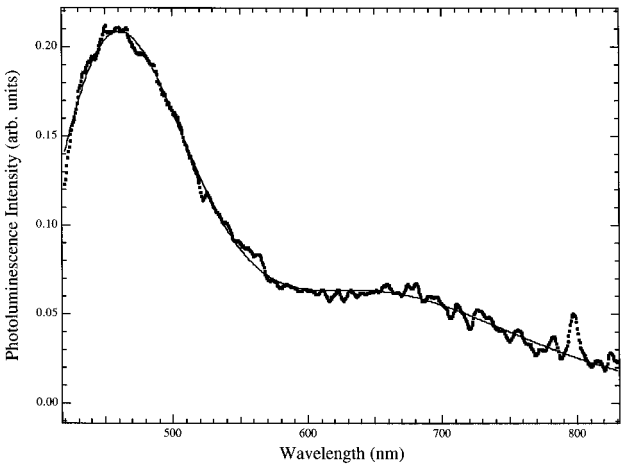

Figure 7. Photoluminescence spectrum of a PS colloid suspension in acetonitrile. Excitation provided by 400 nm laser pulses.

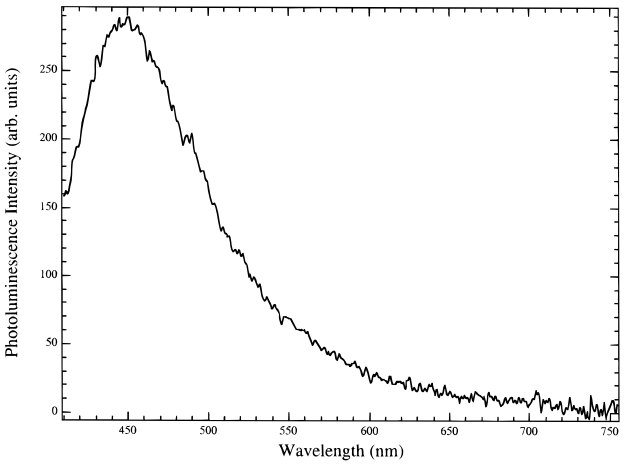

Figure 8. Photoluminescence spectrum of a PS acetonitrile colloid after filtration through 20 nm inorganic sieve. Excitation provided by 400 nm laser pulses.

the Gaussian line shape is appropriate for inhomogeneous broadening arising from the broad range of sizes and shapes expected for the Si nanocrystallites in PS.

Figure 7 shows the PL of a Si colloid suspension (no. 3) in acetonitrile prepared from PS and has a very different spectrum. The relatively low intensity peak in the orange/red region at approximately 680 nm is similar to that observed for PS in Figure 6 but shifted somewhat to higher energy. The broad peak in the blue region centered at 460 nm is quite intense in this spectrum but is not present in the spectrum of as-prepared PS. The spectrum can be easily fit with two Gaussian-shaped peaks. The high-energy peak is similar to the blue peak observed in time-resolved PL studies done on intentionally oxidized PS[22] and supports the conclusions made from the IR data that there is an oxide layer on all of the Si particles despite efforts to minimize exposure to oxygen. In studies done on intentionally oxidized PS, the blue and red peaks coexist at long times,[22] similar to our spectrum taken at low excitation intensities and suggests that Si nanoclusters prepared from PS have a similar level of oxidation. As mentioned above, this is attributed to exposure of the sample to small amounts of O_2/H_2O and perhaps, in addition, the extreme conditions of ultrasonication.

Figure 8 shows the PL spectrum after passing the acetonitrile colloid (no. 7) through the 20 nm sieve. In contrast to Figure 7, it shows no peak in the red region and retains the peak in the blue. This spectrum can be fit quite well with only one Gaussian-shaped peak, and there is no evidence for any contribution from the red. This is consistent with the larger amount of amorphous surface attributed to oxide that is observed in the HRTEM of these samples and suggests that the luminescence from the silicon nanocrystallites within the oxide is simply too weak to be observed. This is also consistent with other studies[22] that show as the oxidation level of the silicon nanoparticles is increased, the red peak diminishes until, at high oxidation levels, only the blue peak is observed.

The origin of the blue PL has yet to be established. Early speculation attributed the blue emission to a direct interband radiative recombination process involving blue-shifted energy levels resulting from quantum confinement. It has also been suggested that the blue PL originates from molecular Si species since the PL decays are exponential and the lifetimes are short and show little dependence on emission wavelength. It is also possible that the blue emission arises from extremely small Si crystallites embedded in an oxide matrix. Small crystallites are required to account for the nanosecond lifetime. This could occur during oxidation just before the Si is consumed. However, there is a growing consensus that it originates from the oxide surface of these particles or from defects in the oxide layer. Further evidence that the blue PL is attributed to the oxide layer is found in the recent synthesis of silica nanoparticles that show bright blue PL.[23−25] The blue PL is attributed to the presence of intrinsic defects of the type $(Si(II))^0$ in the amorphous silica.[26] This blue PL is very similar in peak position and lineshape to what we observe in our Si nanocrystal samples.

Figure 9 shows the dependence of the PL spectrum of an acetonitrile colloid (no. 3) with the excitation intensity. The excitation consisted of 400 nm ∼150 fs laser pulses. The range of excitation intensities extends from <1 mW/cm^2 continuous wave to ∼319 MW/cm^2 peak intensity. The spectra have been normalized to the blue peak heights, and increasing the excitation intensity increases the proportion of the blue peak relative to the red peak. This effect is not permanent and is reversible. This suggests that there may be an interconnection between the emission mechanisms responsible for the two peaks. This phenomenon involves the preferential saturation of the optical transitions responsible for the red peak over the blue peak.

Time resolved lifetime data, which we have presented and discussed in detail in ref 6, show an interesting dependence on the excitation repetition rates and provide insight into this phenomenon. In brief, when low repetition rate excitation (1 kHz) is used, the PL

(22) Kovalev, D. I.; Yaroshetzkii, I. D.; Muschik, T.; Petrova-Koch, V.; Koch, F. *Appl. Phys. Lett.* **1994**, *64*, 214.

(23) Morisaki, H.; Hashimoto, H.; Ping, F. W.; Nozawa, H.; Ono, H. *J. Appl. Phys.* **1993**, *74*, 2977.

(24) El-Shall, M. S.; Turkki, T.; Graiver, D.; Pernisz, U. C.; Baraton, M. I. *J. Phys. Chem.* **1995**, *99*, 17805.

(25) Nozaki, S.; Sato, S.; Ono, H.; Morisaki *Mater. Res. Soc. Symp. Proc* **1994**, *351*, 399.

(26) Skuja, L. N.; Streletsky, A. N.; Pakovich, A. B. *Solid State Commun.* **1984**, *150*, 1069.

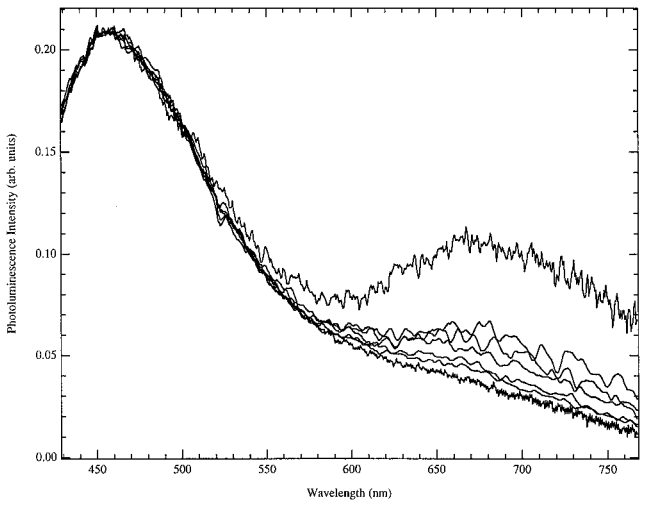

Figure 9. Photoluminescence spectra of a PS colloid in acetonitrile showing the different relative peak heights obtained for different excitation intensities. The intensities increase with decreasing red peak height in the order <1, 16, 32, 51, 101, 160, and 319 MW/cm^2.

decay times are all exponential, short (4.2−5.1 ns) and vary little with emission wavelength. Similar results have been observed by others.[27] With high repetition rate excitation (82 MHz), the red and blue peaks show long-(≥100's ns) and short-(ps−ns) lifetime components. It is conceivable that the short lifetimes observed for both the blue and red emission result from rapid trapping of the excitation at the nanocrystal surface. The long-lifetime component within the blue peak is shorter than its red counterpart and changes little with emission wavelength. This argues against quantum confinement being responsible for this blue component. These lifetimes are more consistent with what would be expected from molecular species, small inclusions of Si or $(Si(II))^0$ defects in the oxide matrix.[22,24,25] In contrast to the blue peak, our results suggest that the red emission results from quantum confinement.[3,21] The red emission peak shows a very long-lived component that can be attributed to the microsecond-decaying red PL component observed in PS and in other Si nanocrystals. The long-lifetime component of the red emission increases as the emission wavelength increases, a trend also seen in PS. This behavior in PS can be interpreted within a variety of models, including quantum confinement. The most successful of these models attributes the dependence of the PL lifetime with emission wavelength and the increased light emission of quantum confined Si to reduced nonradiative recombination processes in PS as compared to bulk Si.[28] This involves the nongeminate recombination of carriers via tunneling from confined zones toward more extended and less passivated regions where nonradiative recombination can occur. This model correctly predicts the PL lifetime variation with emission wavelength in PS.

Though we observe long-lifetime components that have similar wavelength dependencies, their contribution is small. This may be the result of the limited spatial extent of our nanocrystalline system, which fundamentally differentiates it from PS. This would also imply that the colloids we generate contain not only monodispersed nanocrystals but also agglomerated particles similar in morphology to PS. As suggested by the HRTEM, the Si nanocrystals are either monodispersed or aggregated into small clusters of nanocrystals. As a result, tunneling into more extended and less passivated regions is limited at best. Our results suggests that most of the recombination occurs within a single nanocrystal. Our observation of nearly identical nanosecond PL decays (with low repetition rate excitation) throughout the visible suggests that the recombination within the nanocrystal core may occur via localized states in which transport of carriers to these states is the limiting process.

These results also suggest that the blue and red emission originate from different processes. Since the blue transition has a faster emission rate than the red transition,[6] a higher percentage of excitations reaching the states involved in the blue emission will radiatively relax compared to the red emission. At high excitation intensities, the states involved in the red emission will effectively saturate because of the lower emission rate. Consequently, as the excitation intensity increases, more and more emission will originate from the states involved in the blue emission.

Summary

A variety of parameters have been investigated in order to produce PS with crystallites of a uniform morphology. Thin sections of PS are mechanically removed in a drybox under N_2 atmosphere and ultrasonically fractured in distilled, degassed, organic solvents to produce colloids. FTIR spectra show that the starting material is hydrogen passivated, whereas the Si nanoclusters are oxygen passivated. This is attributed to small amounts of O_2/H_2O combined with the extreme conditions of ultrasonication and, perhaps, the length of time the samples are ultrasonicated. HRTEM show that, regardless of previous treatment, the colloids consist primarily of small Si crystallites in the range 2−11 nm and that these crystallites can form agglomerations in solution. An amorphous layer is clearly observed in the large agglomerations by HRTEM. Filtering the colloid through a 20 nm sieve results in agglomerations of Si crystallites with larger amounts of oxide surface. This may be due to increased oxygen exposure when passing through the sieve. PL spectra of the colloids show two peaks, one in the blue which is similar to that observed in silica nanoparticles and one in the red which has been attributed to quantum confinement in Si nanocrystals. In these samples, the lifetime in the red is much shorter than what has been seen in either PS or silicon nanoclusters. The intensities of the two PL peaks are dependent on the excitation intensity and our results suggest that carrier excitations may transfer between the states involved in the blue and red emissions. The peaks originate from different processes within different species and uniform and fast decay times suggest that recombination occurs predominantly within the nanocrystal core via localized states in which transport of carriers to these states is the limiting process. The blue luminescence is probably not due to quantum confinement but may be attributed to $(Si(II))^0$ defects in the oxide matrix.

(27) Tsybeskov, L.; Vandyshev, J. V.; Fauchet, P. M. *Phys. Rev.* **1994**, *49*, 7821.

(28) Vial, J. C.; Bsiesy, A.; Gaspard, F.; Herino, R.; Ligeon, M.; Muller, F.; Romestain, R.; MacFarlane, R. *Phys. Rev. B* **1992**, *45*, 14171.

Acknowledgment. We thank R. L. Smith for the use of the Potentiostat/Galvanostat and R. L. Smith, J. Penczek, and M. L. S. Olsen for useful discussion. We thank C. Nelson and F. Ross for their assistance with the HRTEM. This work was supported by the Director, Office of Energy Research, Office of Basic Energy Sciences, US Department of Energy under Contract No. DE AC-03-76SF00098 and by the National Science Foundation (DMR-9201041), and performed under the auspices of the U. S. Department of Energy by Lawrence Livermore National Laboratory under contract No. W-7405-ENG-48.

CM950608K